A COMPUTATIONAL TOOL FOR THE DESIGN OF ULTRASONIC SYSTEMS

S. J. Wormley, D. O. Thompson and K. M. Lakin
Ames Laboratory-USDOE
Iowa State University
Ames, IA 50011

I. INTRODUCTION

Advances in elastic wave scattering and inversion techniques have shown that advances in transducer technology are needed in order to fully exploit them. This is particularly true in the case of flaw sizing algorithms in which it has been demonstrated that a need exists for transducers with specified bandwidth characteristics. As a part of an effort to develop a composite, multiviewing ultrasonic transducer for flaw characterization, a computational tool has been developed which provides a convenient way to select driver pulse shapes and transducer characteristics which optimize this property. The purpose of this paper is to discuss this computational tool.

Work has been done by Mason [1] and others in the development of equivalent circuit representation of transducers. Mason's model, in particular, is used in this work. Jayosundere and Bond [2] have also recently studied transducer properties, and Yu, Ilic, Khuri-Yakub, Kino [3,4] pioneered work with unipolar transducers and unipolar stress pulses. Work done by Doctor et al. indicates that a square wave driving waveform reduces the need to tailor the waveform and eliminates distortions caused by exponential decay, thus providing improved near surface resolution and improved reproducibility [5].

II. MODEL SIMULATION AND IMPLEMENTATION

As shown initially by Mason [1], equivalent circuits in which properties of piezoelectric crystals are expressed in terms of equivalent elements, are often useful. The elements are combinations of inductors, capacitors and resistors. By adding electrical

or mechanical elements it is often possible to make the circuits into the form of filter sections which can be designed to match the electrical and mechanical conditions of the driving and receiving end. Mason shows that a transducer with backing can be represented as a 3 port device; one electrical port and two mechanical ports, one on each side of the transducer. This can be reduced to a two port representation by pulling the backing "inside" the model, resulting in a model with one electrical port and one mechanical port (Fig. 1).

This model can then be represented by two-port network theory. In this case, the mechanical and electrical systems are represented as combinations of series and parallel two-port networks and connected by a transmission-parameter matrix. The transmission-parameter matrix of a cascade of two-port networks is equal to the matrix product of transmission parameter matrices of the two-port networks. Thus,

$$T \equiv \begin{bmatrix} A & B \\ C & D \end{bmatrix}_T = \prod_{n=1}^{N} (T_n) \qquad (1)$$

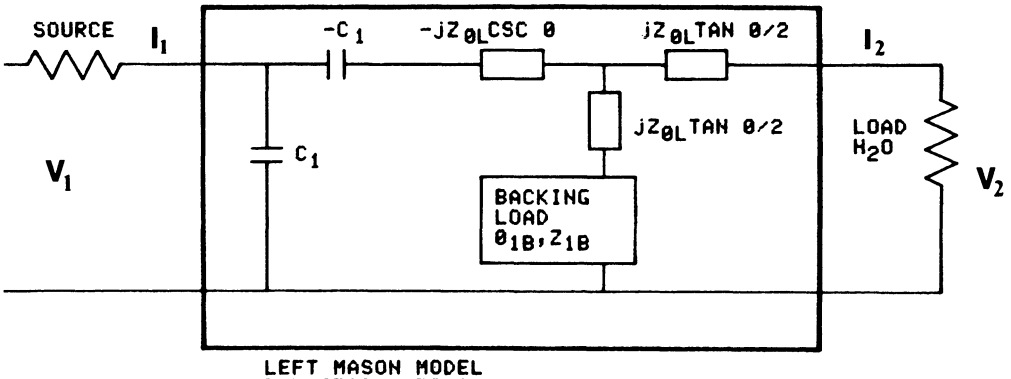

Fig. 1. Mason's model block diagram for an immersion transducer, which is conveniently represented by two series and two parallel transmission-parameter matricies. The driver pulse series resistance is a property of the driving electronics.

The input and output voltages and currents are then related by

$$\begin{bmatrix} V_1 \\ I_1 \end{bmatrix} = \begin{bmatrix} A & B \\ C & D \end{bmatrix}_T \begin{bmatrix} V_2 \\ -I_2 \end{bmatrix} . \tag{2}$$

The transfer function for the resultant two-port network at a single frequency [6] is then given by

$$T = \left[\begin{array}{cc|cc} A_r & B_r & -A_i & -B_i \\ C_r & D_r & -C_i & -D_i \\ \hline A_i & B_i & A_r & B_r \\ C_i & D_i & C_r & D_r \end{array}\right] \tag{3}$$

and the input/output ratio is

$$V_1/V_2 = \frac{R_L(T_{11}\,R_L+T_{22}) - jR_L(T_{31}\,R_L+T_{32})}{(T_{11}\,R_L+T_{12})^2 + (T_{31}\,R_L+T_{32})^2} . \tag{4}$$

For the work done here, the transfer function is computed at 256 discrete frequencies and takes the form of a 512 point array, with 256 pairs of real and imaginary components representing frequencies from DC to 2 F_o where F_o is the characteristic frequency at the transducer being modeled.

The impulse response, H(t) is the time domain response of the transducer model to a delta function and is determined by performing an inverse Fast Fourier Transform (IFT) on the transfer function $H(\omega)$

$$H(t) = (1/N) \sum_{\omega=0}^{N-1} H(\omega)e^{j2\pi nk/N} \quad \text{for } n=0,1,---,N-1 \tag{5}$$

The resultant mechanical waveform G(t) produced in the water is then the convolution of the driving function F(t) and the Mason model impulse response H(t):

$$G(t) = F(t) * H(t), \text{ or} \tag{6}$$

$$G(t) = \sum_{t=0}^{N-1} F(t)H(n-t) \text{ for } n=0,1,---,2N-2. \quad (7)$$

III. EXAMPLES OF RESULTS

Model parameters, i.e., size, backing, frequency and material, were selected to approximate existing commercial transducers in the laboratory. The parameters specified are:

Piezoelectric Material (PZT_4)
- velocity - 6.00×10^5 cm/sec
- coupling coefficient - 0.68

Frequency (thickness) - 10 MHz (3×10^{-2} cm)
Piezoelectric diameter - 0.25 inches
Backing material
- length - 0.48 cm (8λ)
- attenuation - 10 nep/cm

A. Forward Problem

1. Several examples are shown for various driving functions studied. The simplest case is that of a spike driving function, shown in Fig. 2, which exhibits a DC component and excellent low frequency density (Fig. 3). Upon convolution with the Mason model impulse response H(t) (Fig. 4) the resulting response in a water bath is shown in both time and frequency domains (Figs. 6,7).

A second driver waveform that has been examined is shown in Fig. 8. As the width of the negative portion of the pulse was varied, variations in the spectral response through the Mason model are observed (Fig. 9). By holding the delta T to the minimum duration resolveable by the computer algorithm, the effect of the undershoot size was studied (Figs. 10,11). It is evident that considerable control exists in the "shaping" of spectral response by selection of the duration and extent of the negative portion of this composite step function.

2. Effects of Backing

Backing in the Mason model is defined in terms of the impedance Z_{LB} and phase θ_{LB}. The backing phase is of the form

$$\theta_{LB} = \beta\ell + j\alpha\ell \quad (8)$$

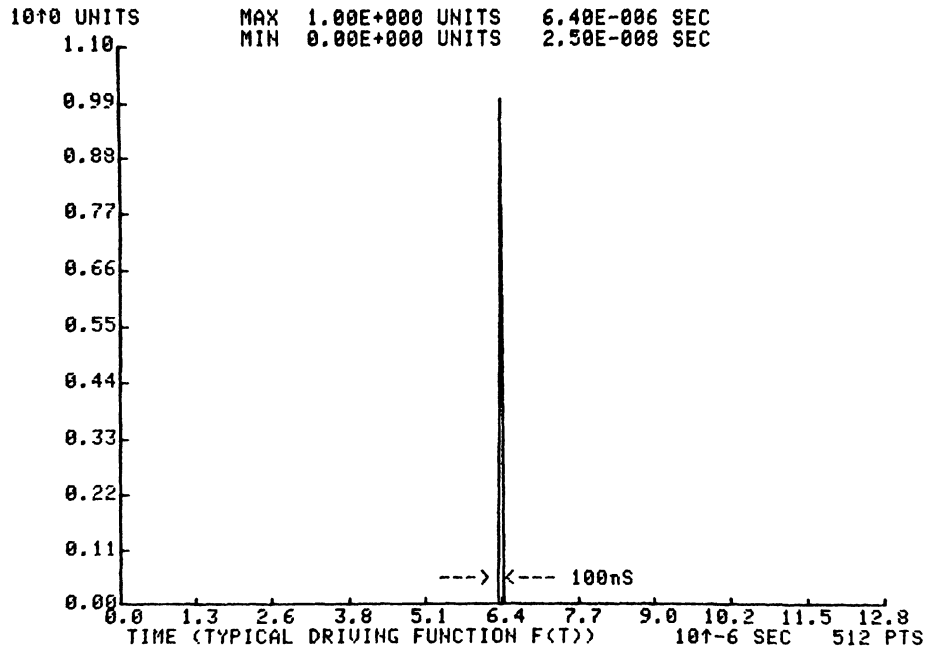

Fig. 2. Computer generated "spike" driving function. Some commercial ultrasonic pulsars approach, but do not achieve the ideal spike without undershoots, thus reducing the lower frequency content.

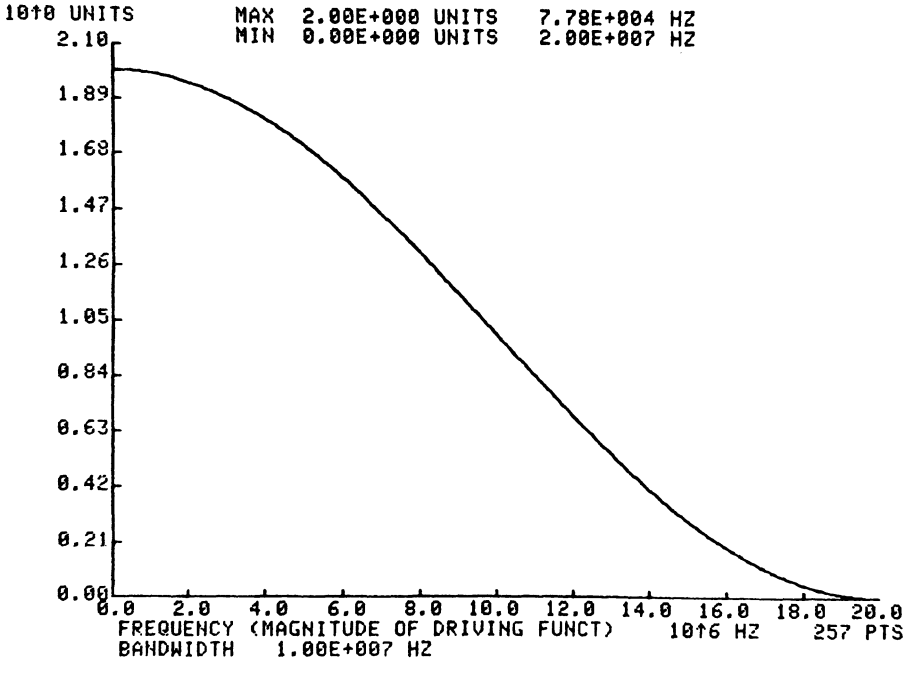

Fig. 3. Frequency response of computer generated "spike."

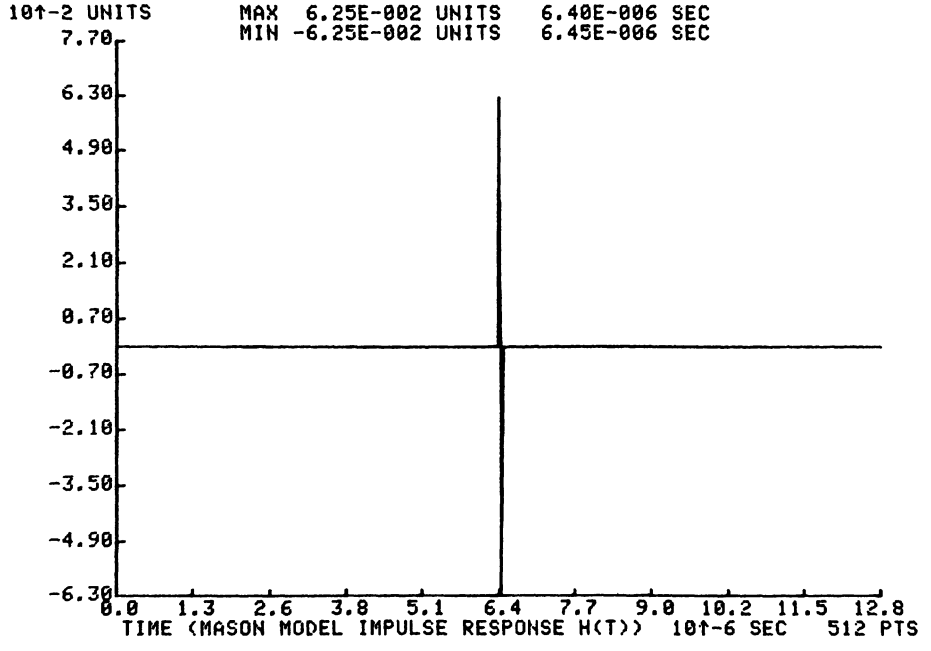

Fig. 4. Impulse response of Mason model, cintered in time window. Load impedance: 8.8 ohms (water).

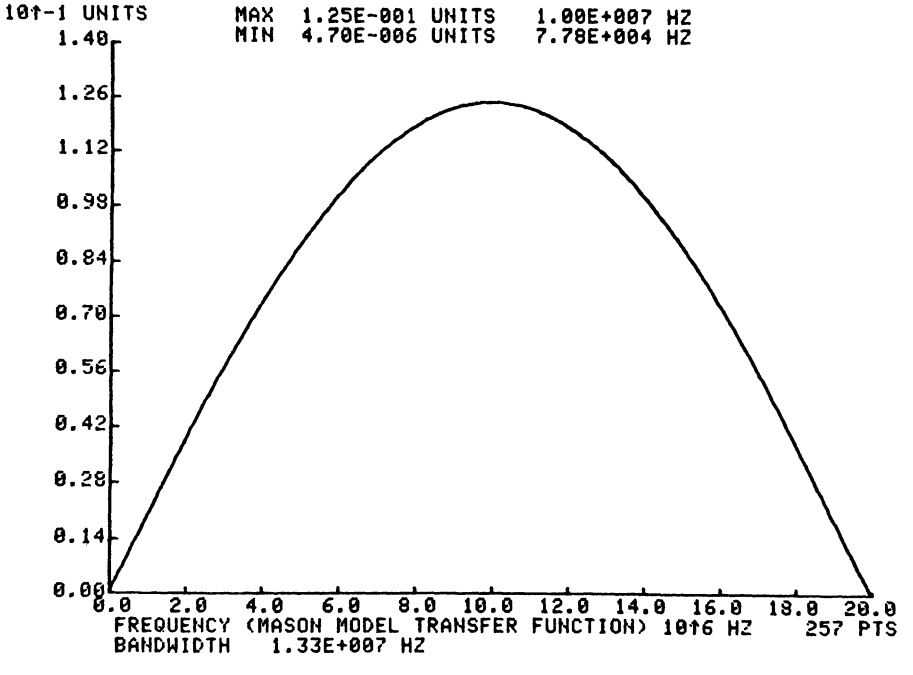

Fig. 5. Transfer function of Mason model. Load impedance: 8.8 ohms. (water).

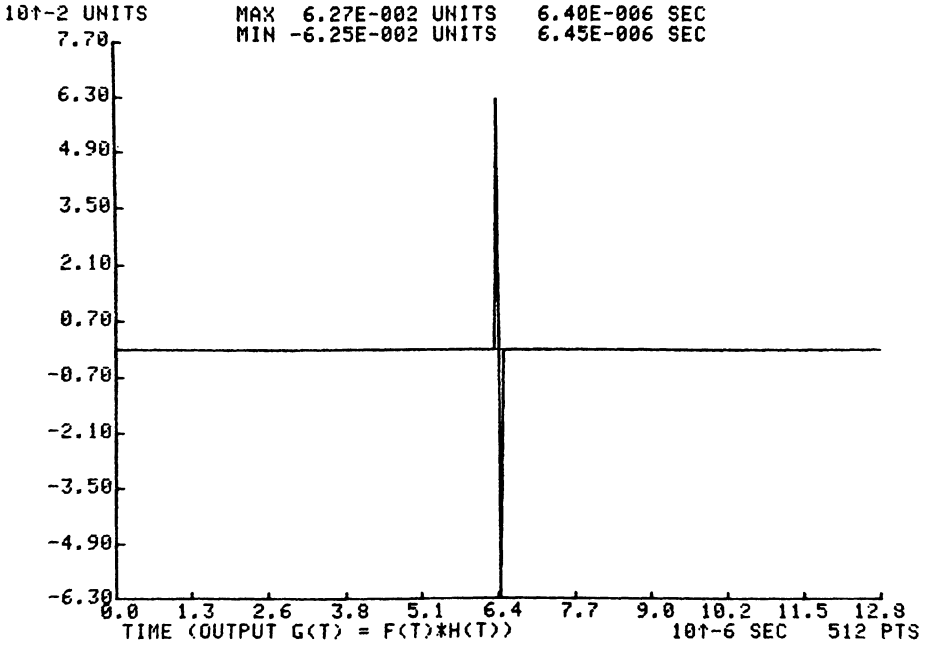

Fig. 6. Convolution of computer generated "spike" driving function and Mason model impulse response.

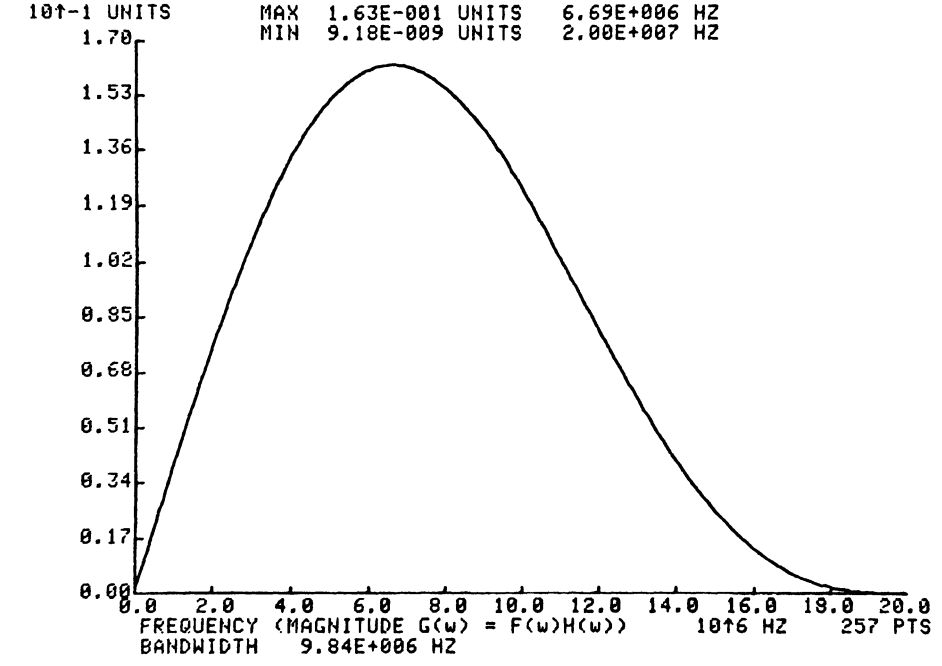

Fig. 7. Frequency domain representation of convolution typical of many commercial ultrasonic pulsars.

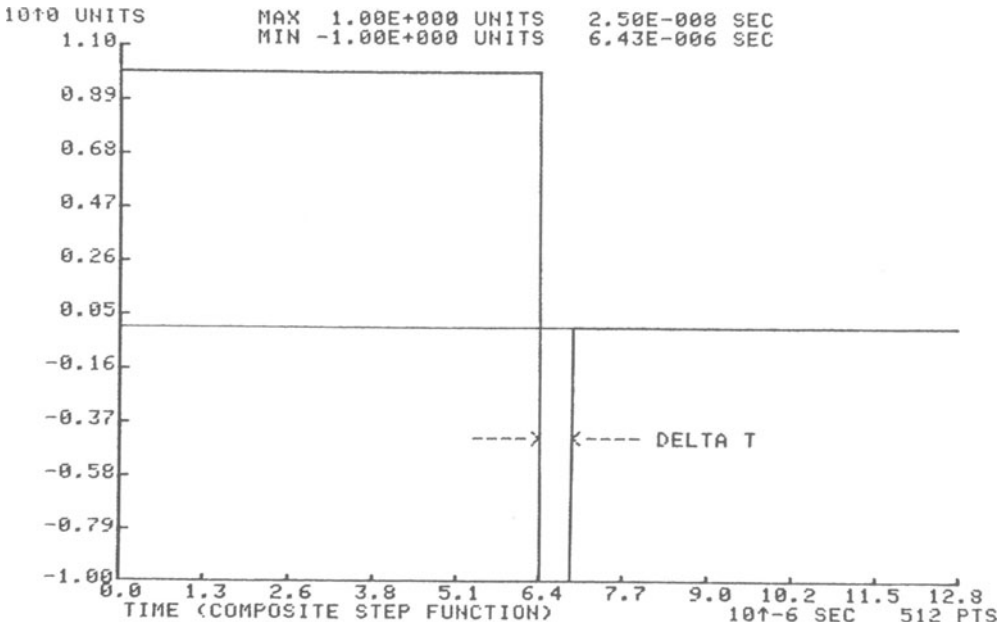

Fig. 8. Computer generated driving function - composite step, becoming a bipolar step function as delta T increases.

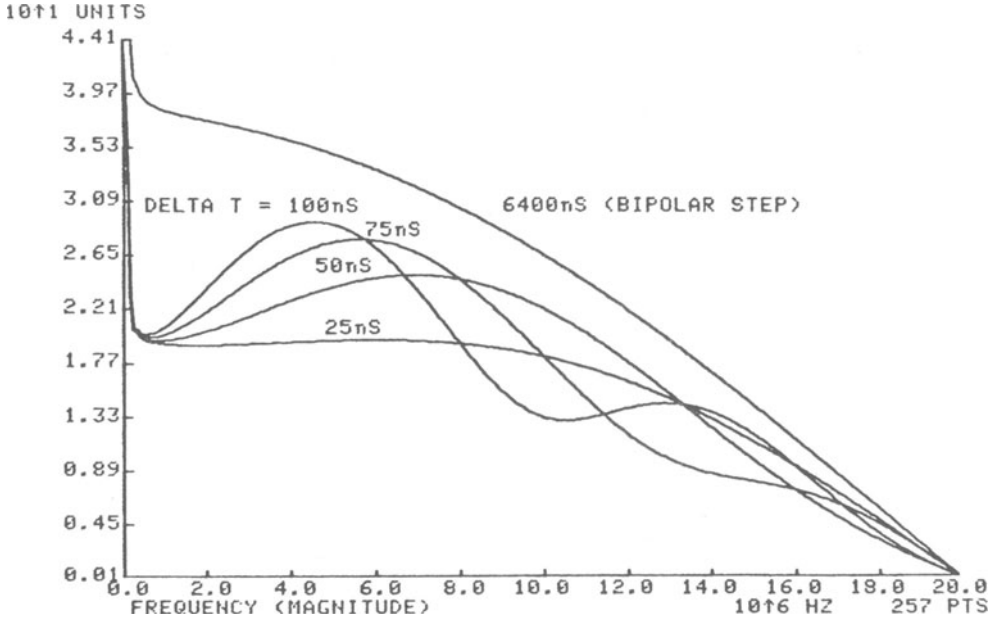

Fig. 9. Frequency response of composite step function convolved with Mason model impulse response for various delta T. Modulation increases as delta T increases. A 50% Hanning window was used on bipolar step response to show modulation average.

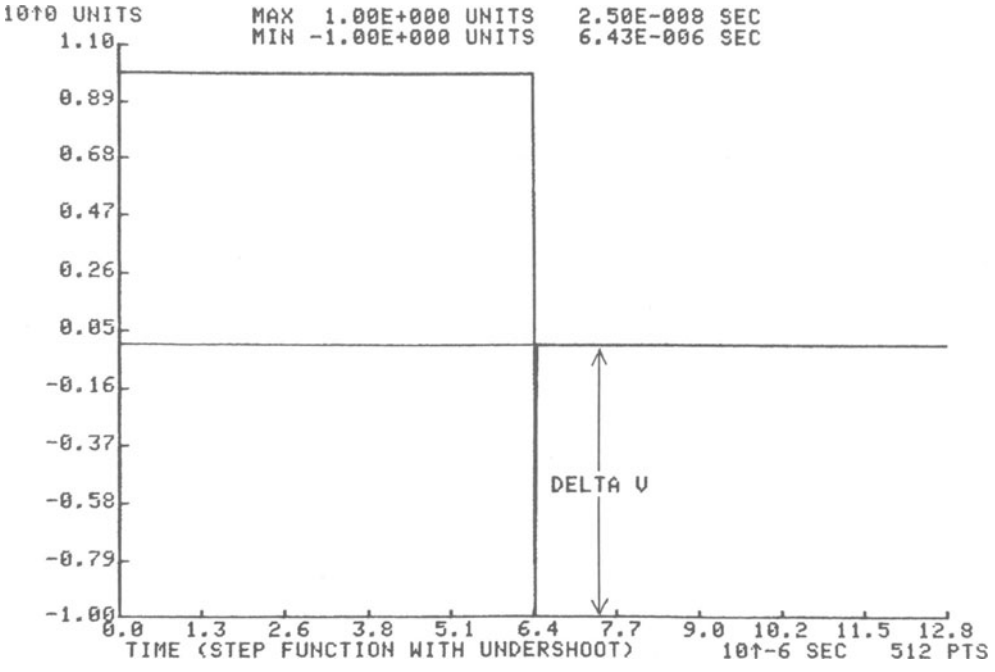

Fig. 10. Computer generated driving function - unipolar step with undershoot.

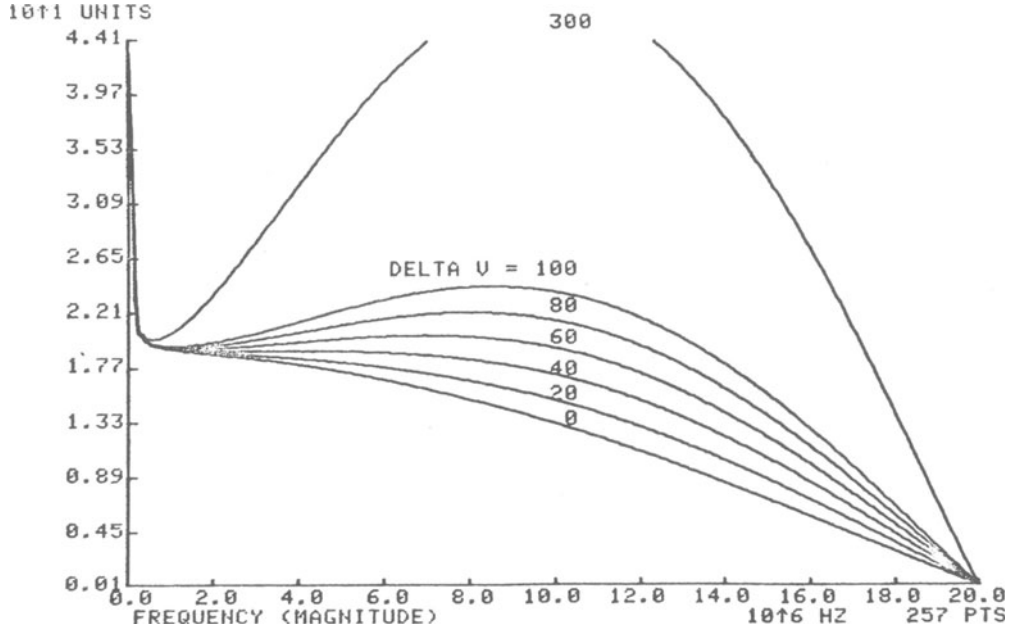

Fig. 11. Frequency response of unipolar step with undershoot convolved with Mason model impulse response for various delta V.

in which α and ℓ are the attenuation and thickness of the backing material, and β is the propagation constant in the backing material given by

$$\beta = \frac{2\pi}{\lambda_B} = \frac{2\pi f}{V_B} . \tag{9}$$

The attenuation α is specified in nepers/cm and the length of backing in multiples of the piezoelectric wavelength λ.

The spectral responses (driven by a delta function) for the transducer model are shown in Fig. 12 for various backing impedances as a percentage of the piezoelectric material impedance. Lower backing impedance narrows the response about the characteristic center frequency F_o. Higher backing impedance tends to increase resonances at integral multiples of $F_o/2$.

In Fig. 13, the backing length was held constant at 16 half wavelengths and attenuation varied. Reflected unabsorbed energy causes interference in the piezoelectric which show up as modulation in the frequency spectrum. Within the resolution of the computer model, the energy in the backing was completely absorbed as the attenuation approached 8 nep/cm.

B. Inverse Problem

There would be an obvious advantage if a transducer driving function H(t) could be determined from a specified output transducer function $G(\omega)$. Our approach to this inverse problem is to deconvolve the transducer characteristics, $H(\omega)$ from the predetermined spectral output $G(\omega)$.

$$F(\omega) = \frac{G(\omega)}{H(\omega)} = \frac{G(\omega)\ \bar{H}(\omega)}{(H(\omega))^2} \tag{12}$$

The deconvolution process is sensitive to both noise and the effects of windowing. Figure 14 shows one possibility for an "ideal" spectral response. By deconvolving $H(\omega)$ (see Fig. 7) from $G(\omega)$, the result transformed into the time domain is shown in Fig. 15.

IV. CONCLUSIONS

This computer modeling is preliminary and will be developed further as part of ongoing work. It has been demonstrated that experimental results can be duplicated with the mode, and that it is useful in guiding selections of transducer pulse driver shapes in order to obtain extended bandwidth performance. The model can

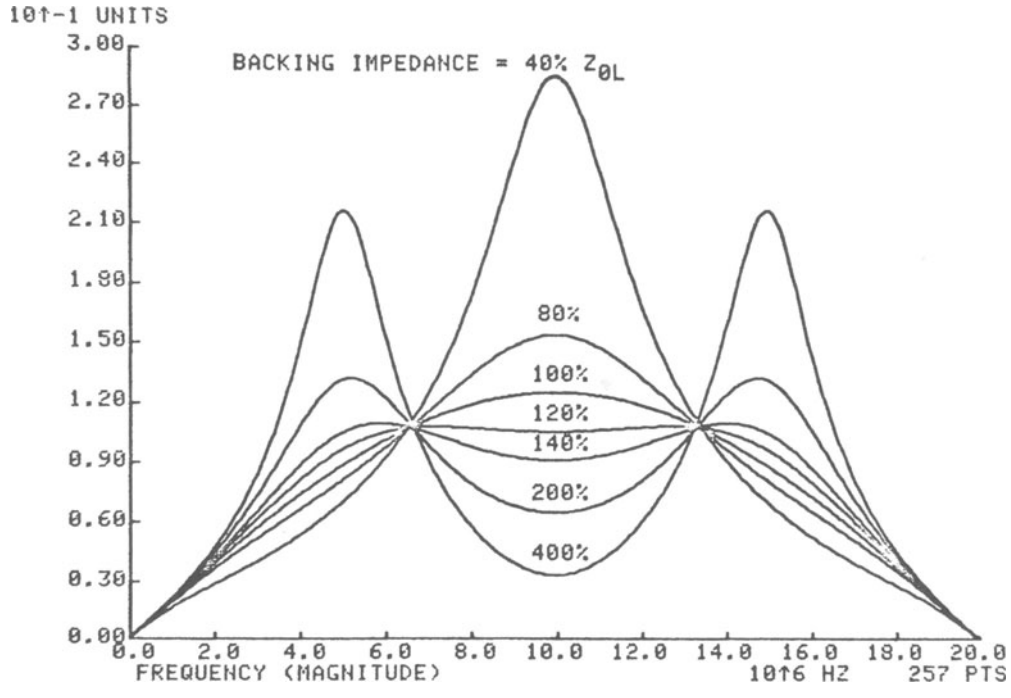

Fig. 12. Mason model transfer function - backing impedance as a percentage of piezoelectric material impedance.

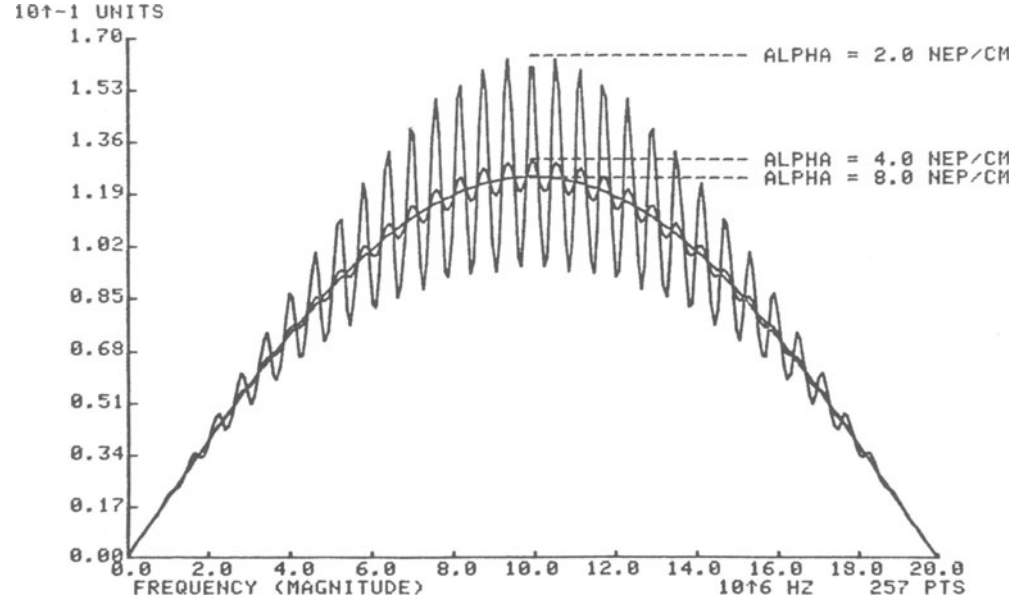

Fig. 13. Mason model transfer function - backing attenuation.

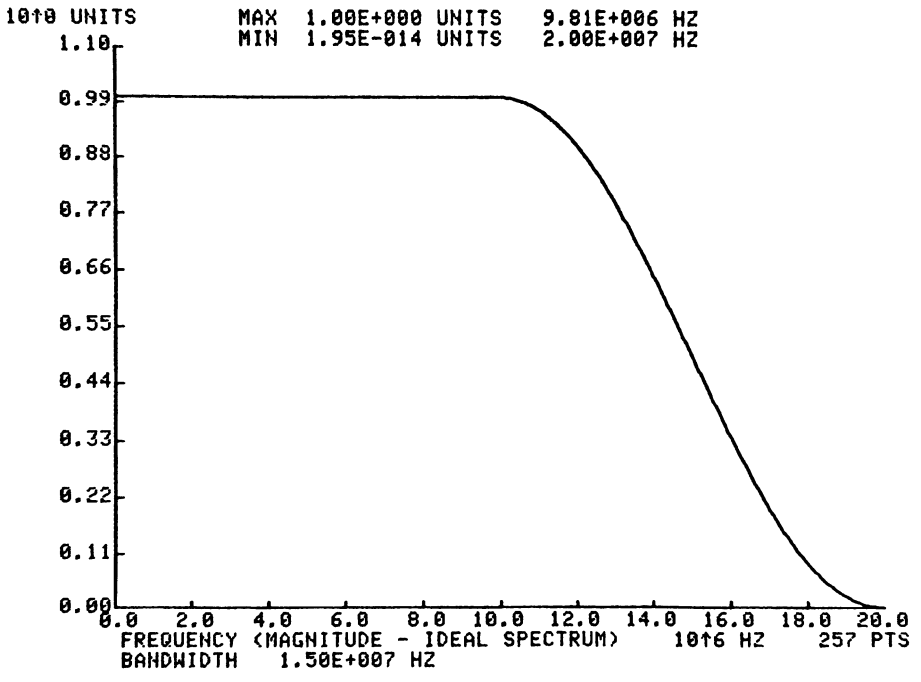

Fig. 14. "Ideal" spectral response of driver function and ultrasonic transducer.

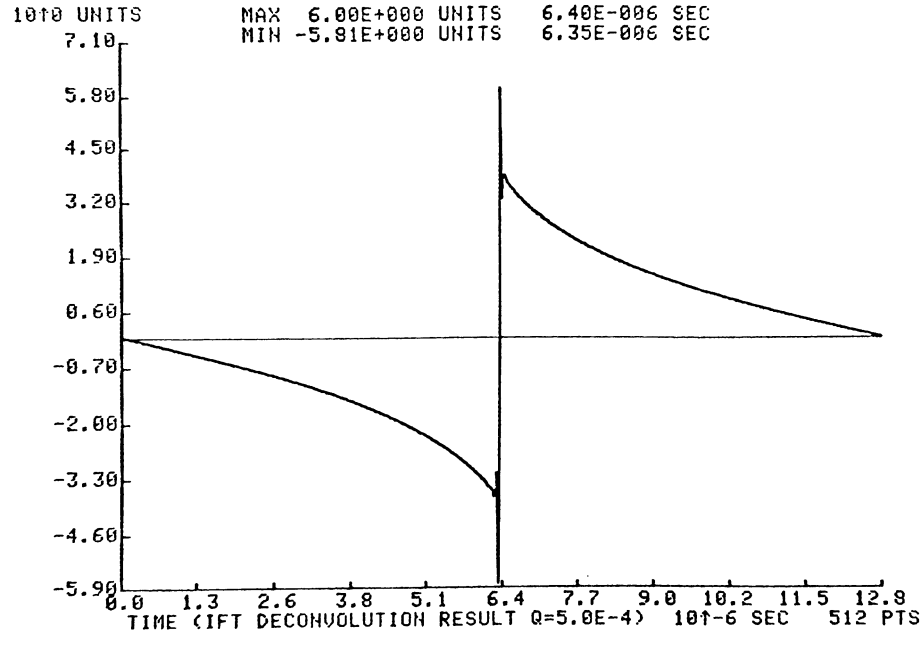

Fig. 15. "Ideal" transducer driving function as predicted by the Mason model - inverse mode.

be expanded to include two transducers in pitch-catch modes and can include characteristics of receiver and driver electronics as part of an effort to insure an optimal spectral response. Preliminary consideration has been given to using it in an inverse mode, i.e., to specify the spectral bandwidth desired from the transducer and to determine the driver pulse required. Determination of $H^{-1}(t)$ may possibly be solved by application of constrained linear inversion techniques [7], however, determination of F(t) may be reasonably approximated using deconvolution techniques.

ACKNOWLEDGEMENT

The Ames Laboratory is operated for the U.S. Department of Energy by Iowa State University under Contract No. W-7405-ENG-82. This work was supported by the Director of Energy Research, Office of Basic Energy Sciences.

REFERENCES

1. W. P. Mason, Physical acoustics and the properties of solids, Van Nostrand (1958).
2. N. Jayasundere and L. J. Bond, Ultrasonic transducer standards, these proceedings (1982).
3. F. Yu, D. B. Ilic, B. T. Khuri-Yakub, and G. S. Kino, Appl. Phys. Lett. 36(7), 553 (1980).
4. F. Yu, D. B. Ilic, B. T. Khuri-Yakub, and G. S. Kino Ultrasonics Symposium, 284 (1979).
5. S. R. Doctor, A. G. Gibbs, and R. P. Gribble, Waveform design for maximum pass-band energy, Pacific Northwest Laboratories, (1979).
6. L. T. Huelsman, Circuits, matrices and linear vector spaces, Mc-Graw-Hill (1963), p. 44-111.
7. S. Twomey, Introduction to the mathematics of inversion in remote sensing and direct measurements, Elsevier Scientific Publ. Co. (1980).